A El-Moniem M. Amin et al. Int. Journal of Engineering Research and Applications www.ijera.com
ISSN: 2248-9622, Vol. 6, Issue 1, (Part - 3) January 2016, pp.72-78

RESEARCH ARTICLE OPEN ACCESS

Assessment the Limit of Steel Core Area in the Encased Composite Column

Abd El-Moniem M. Amin[1]; Ashraf M. Fadel[2]; Sameh M. Gaawan[3]; Reda A. Darwish[4]

[1] Professor, Dept. of Civil Engineering, Univ. of Helwan, Egypt.
[2] Professor, Institute of Structures and Metallic Construction, HBRC, Egypt.
[3] Associate Professor, Dept. of Civil Engineering, Univ. of Helwan, Egypt.
[4] Postgraduate student, Dept. of Civil Engineering, Univ. of Helwan, Egypt.

Abstract
This study has been carried out to evaluate the method of design of the composite column of reinforced concrete and steel structural sections in the international Codes. Studying and verifying the limit of the ratio of steel section area to total gross section area is the important aim of this research. AISC, 2005 was specifying this limit by 1.0%. Various ratios of steel core area to total gross section area were studied along with rang of concrete strength by the help of finite element software. The results show that the ratio of the steel core area to the total gross section area (A_s/A_g) should be replaced by the ratio of the ultimate capacity of the steel core to the total ultimate capacity of the complete composite section (P_{ys}/P_0). The new ratio takes into account the effect of relative strength between steel and concrete. The proposed limit for (P_{ys}/P_0) is between (25%) to (30%).
Keywords: *Composite column; Encased section; Steel; Concrete; Finite element method*

I. Introduction:

According to American Institute of Steel Construction AISC (LRFD), 2005 there are five limits should be satisfied by any column section to be covered by this code. The ratio of the steel core area to the gross section area is one of the important limitations specifying the range of code work. The code limit the As/Ag by 1.0% thus the composite columns sections with As/Ag less than 1.0% should be designed as a normal reinforced concrete column and the steel core will work as concentrate steel reinforcement consequently these columns will follow the terms and clauses of the ACI code.
This limit will be assessed by studying the results of the finite element models and compare them with the capacity of these section based on AISC

II. Finite Element Models

Sixty models have been performed to study the effect of the steel core area ratio to the total gross section area of the encased section.
The model naming convention reflects the steel ratio and concrete strength e.g., (C-6.58-35) refers to a section with a steel core ratio of A_s/A_g = 6.58% and concrete strength = 35Mpa).
All the models have the same cross section as illustrates in adjacent figure.

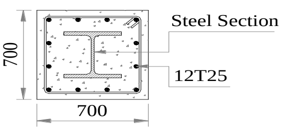

Variables Considered

Generally there are number of variables governing the capacity of the encased column sections such as; the height of the column, the dimensions of the concrete encasement, the area of the steel reinforcement, the area of the steel core, the strength of the concrete encasement, the strength of steel core and the strength of the steel reinforcement bars. The variables considered in this study are the area of the steel Core and the strength of the concrete encasement. The other variables are assumed to be constant.
Values of these constant variables shown in tables (1) & (2).

Property	Description	Value	Units
EX	Elasticity Modulus	200,000	Mpa
NUXY	Poisson's ratio in XY	0.3	Dimension Less
SIGYLD	Yield Stress	345	Mpa
ETAN	Tangent Modulus	4200	Mpa
DENS	Mass Density	7850	Kg/m3

Table (1) Steel Material Properties

Property	Description	Value	Units
NUXY	Poisson's ratio in XY	0.2	Dimension Less
DENS	Mass Density	2400	Kg/m3

Table (2) Concrete Material Properties

The values of the stress-strain curve of concrete material are based on smeared crack approach. We can summarize the curve for each group as shown in tables (3) & (4) and figure (1) and the smeared crack approach as illustrate in table (6).

Group (1) f_c' = 25 (Mpa)		Group (2) f_c' = 30 (Mpa)		Group (3) f_c' = 35 (Mpa)	
ε x 10^{-3}	σ Mpa	ε x 10^{-3}	σ Mpa	ε x 10^{-3}	σ Mpa
-0.13	-3.2	-0.13	-3.5	-0.13	-3.7
0.32	7.5	0.35	9.0	0.38	10.5
0.77	16.0	0.84	19.2	0.91	22.4
1.22	21.6	1.33	25.9	1.44	30.2
1.66	24.3	1.82	29.2	1.97	34.0
2.11	25.0	2.32	30.0	2.50	35.0

Table (3) Concrete Stress-Strain Values for (Groups 1, 2 & 3)

Group (4) fc' = 40 (Mpa)		Group (5) fc' = 45 (Mpa)		Group (6) fc' = 50 (Mpa)	
ε x 10^{-3}	σ Mpa	ε x 10^{-3}	σ Mpa	ε x 10^{-3}	σ Mpa
-0.13	-4.0	-0.13	-4.2	-0.13	-4.5
0.40	12.0	0.43	13.5	0.45	15.0
0.97	25.6	1.03	28.8	1.08	32.0
1.54	34.6	1.63	38.9	1.72	43.2
2.11	38.9	2.23	43.7	2.35	48.6
2.67	40.0	2.84	45.0	2.99	50.0

Table (4-4) Concrete Stress-Strain Values for (Groups 4, 5 & 6)

The models have been divided to six groups each group have different concrete strength (25, 30, 35, 40, 45, and 50 Mpa). Each group has ten specimens with different steel section profiles to produce a range of As/Ag from 0.57% to 9.76 as shown in tables (5).

	Model Name	Steel Section	As mm^2	As/Ag %
1	C-0.57-25	W10x15	2800	0.58
2	C-0.86-25	W10x22	4200	0.85
3	C-1.00-25	W10x26	4900	1.00
4	C-1.16-25	W10x30	5700	1.16
5	C-2.55-25	W10x66	12500	2.55
6	C-3.35-25	W10x89	16900	3.45
7	C-5.24-25	W12x136	25700	5.25
8	C-6.59-25	W12x170	32300	6.58
9	C-8.14-25	W12x210	39900	8.14
10	C-9.76-25	W12x252	47800	9.76

Table (5) As/Ag for specimens of each groups

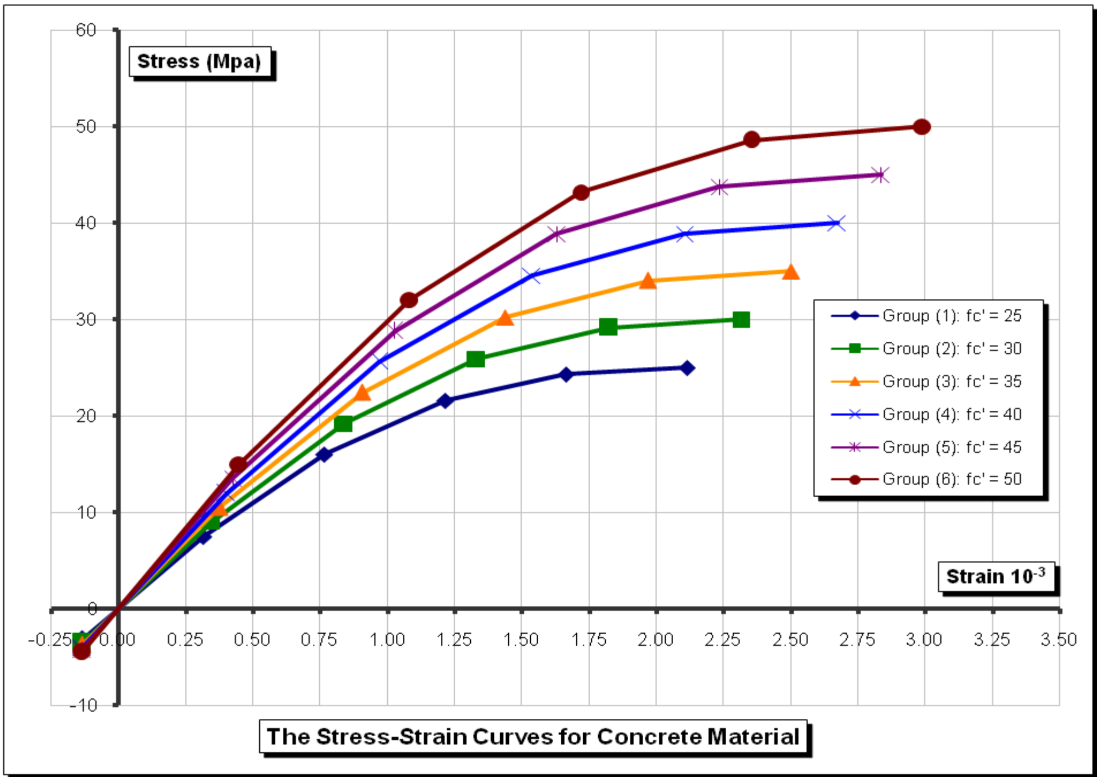

Figure (1) shows the stress-strain curves for all groups.

The Strain (ε)		The Stress (σ)	
ε_T	$= f_T/E_c = 1.32\ e^{-4}$	f_T	$= 0.632 \sqrt{f_c'}$
ε_E	$= f_E/E_c = 6.34\ e^{-5} (\sqrt{f_c'})$	f_E	$= 0.3\ f_c'$
ε_1	$= \varepsilon_E + ¼ (\varepsilon_0 - \varepsilon_E)$	f_1	$= (E_c.\varepsilon_1)/(1+(\varepsilon_1/\varepsilon_0)^2)$
ε_2	$= \varepsilon_E + ½ (\varepsilon_0 - \varepsilon_E)$	f_2	$= (E_c.\varepsilon_2)/(1+(\varepsilon_2/\varepsilon_0)^2)$
ε_3	$= \varepsilon_E + ¾ (\varepsilon_0 - \varepsilon_E)$	f_3	$= (E_c.\varepsilon_3)/(1+(\varepsilon_3/\varepsilon_0)^2)$
ε_0	$= 2.f_c'/E_c = 4.23\ e^{-4} (\sqrt{f_c'})$	f_c'	
Since, $E_c = 4730 \sqrt{f_c'}$			

Table (6) Stress-Strain equations based on the smeared crack approach

III. Results and Discussions

A nonlinear analysis had been performed for all the models to get the failure load ($P_{,FE\ Model}$), and in same time the maximum capacity load according to AISC-LRFD, 2005 ($P_{n,\ AISC}$) had been calculated.

The results of both ($P_{,FE\ Model}$) & ($P_{n,\ AISC}$) for each group are tabulating against two reference values as shown in tables (7) & (8) and figures from (2) to (14):

1. The ratio of the steel core area to the total gross section area (As/Ag)
2. The ratio of the ultimate capacity of the steel core to the total ultimate capacity of the complete composite section (P_{ys}/P_0) (Where; P_{ys} = As. F_y and P_0 = As . F_y + A_{sr} . F_{yr} + 0.85f_c'.Ac)

For each group the range of (As/Ag) values will be the same (0.57, 0.86, 1.00, 1.16, 2.55, 3.35, 5.24, 6.59, 8.14 & 9.76%).

However, the range of (P_{ys}/P_0) values for each group will be function of the concrete strength, which differs from group to group.

As / Ag	Group (1)		Group (2)		Group (3)		Group (4)		Group (5)		Group (6)	
	$P_{n,AISC}$ (KN)	$P_{,FE\ Model}$ (KN)	$P_{n,AISC}$ (KN)	$P_{,FE\ Model}$ (KN)	$P_{n,AISC}$ (KN)	$P_{,FE\ Model}$ (KN)	$P_{n,AISC}$ (KN)	$P_{,FE\ Model}$ (KN)	$P_{n,AISC}$ (KN)	$P_{,FE\ Model}$ (KN)	$P_{n,AISC}$ (KN)	$P_{,FE\ Model}$ (KN)
0.57%	9,721	11,763	10,902	13,455	11,935	14,890	12,993	16,484	13,812	17,573	14,633	18,713
0.86%	9,860	11,685	11,043	13,347	12,069	14,728	13,074	16,145	13,999	17,443	14,928	18,824
1.00%	10,008	11,829	11,202	13,505	12,258	14,946	13,125	16,006	13,939	17,011	14,745	18,063
1.16%	10,171	11,992	11,375	13,680	12,336	14,873	13,313	16,185	14,166	17,264	14,954	18,249
2.55%	11,304	12,378	12,563	14,031	13,930	16,006	14,993	17,351	15,943	18,492	16,922	19,751
3.45%	12,099	12,922	13,396	14,593	14,582	16,084	15,566	17,182	16,859	19,015	17,804	20,117
5.24%	14,579	15,541	16,019	17,418	17,165	18,708	18,295	20,006	19,568	21,658	20,591	22,796
6.59%	16,339	17,499	17,877	19,530	19,074	20,887	20,279	22,291	21,478	23,718	22,572	24,949
8.14%	18,221	19,405	19,827	21,538	21,086	22,967	22,344	24,431	23,541	25,796	24,672	27,046
9.76%	20,310	21,651	22,000	23,921	23,183	25,140	24,514	26,715	25,782	28,188	26,975	29,521

Table (7) The Results of all groups (1 of 2)

As / Ag	Group (1)		Group (2)		Group (3)		Group (4)		Group (5)		Group (6)	
	P_{ys} / P_0	$P_{,FE\ Model}$ / $P_{n,AISC}$	P_{ys} / P_0	$P_{,FE\ Model}$ / $P_{n,AISC}$	P_{ys} / P_0	$P_{,FE\ Model}$ / $P_{n,AISC}$	P_{ys} / P_0	$P_{,FE\ Model}$ / $P_{n,AISC}$	P_{ys} / P_0	$P_{,FE\ Model}$ / $P_{n,AISC}$	P_{ys} / P_0	$P_{,FE\ Model}$ / $P_{n,AISC}$
0.57%	0.071	1.210	0.062	1.234	0.055	1.248	0.049	1.269	0.044	1.272	0.040	1.279
0.86%	0.103	1.185	0.090	1.209	0.080	1.220	0.072	1.235	0.065	1.246	0.060	1.261
1.00%	0.118	1.182	0.103	1.206	0.092	1.219	0.083	1.220	0.075	1.220	0.069	1.225
1.16%	0.135	1.179	0.118	1.203	0.106	1.206	0.095	1.216	0.087	1.219	0.079	1.220
2.55%	0.257	1.095	0.230	1.117	0.208	1.149	0.189	1.157	0.174	1.160	0.161	1.167
3.45%	0.320	1.068	0.289	1.089	0.263	1.103	0.241	1.104	0.223	1.128	0.207	1.130
5.24%	0.421	1.066	0.386	1.087	0.355	1.090	0.330	1.094	0.307	1.107	0.288	1.107
6.59%	0.481	1.071	0.444	1.092	0.412	1.095	0.385	1.099	0.361	1.104	0.340	1.105
8.14%	0.537	1.065	0.500	1.086	0.468	1.089	0.440	1.093	0.415	1.096	0.392	1.096
9.76%	0.585	1.066	0.549	1.087	0.517	1.084	0.488	1.090	0.463	1.093	0.440	1.094

Table (8) The Results of all groups (2 of 2)

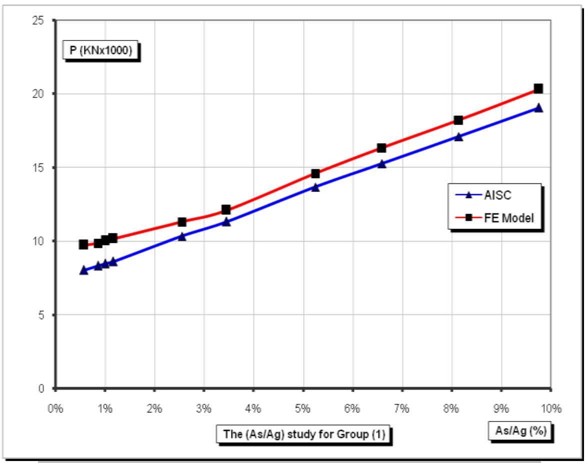

Figure (2) shows the result of study (A_s/A_g) for Group (1)

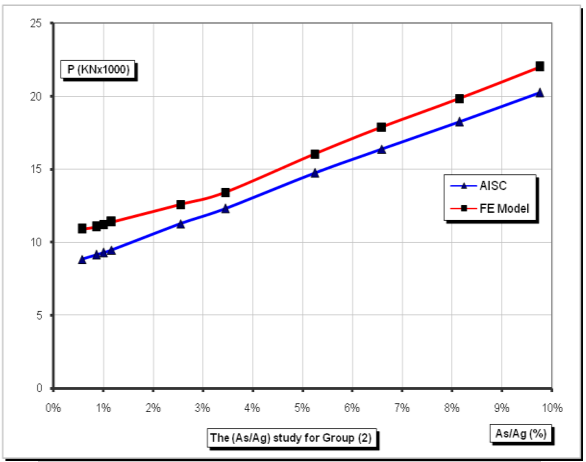

Figure (3) shows the result of study (A_s/A_g) for Group (2)

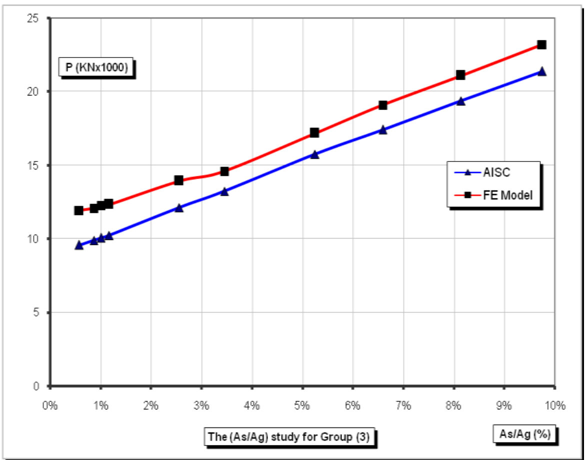

Figure (4) shows the result of study (A_s/A_g) for Group (3)

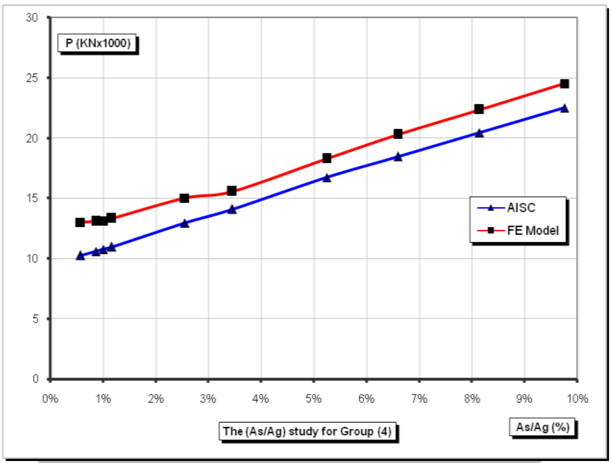

Figure (5) shows the result of study (A_s/A_g) for Group (4)

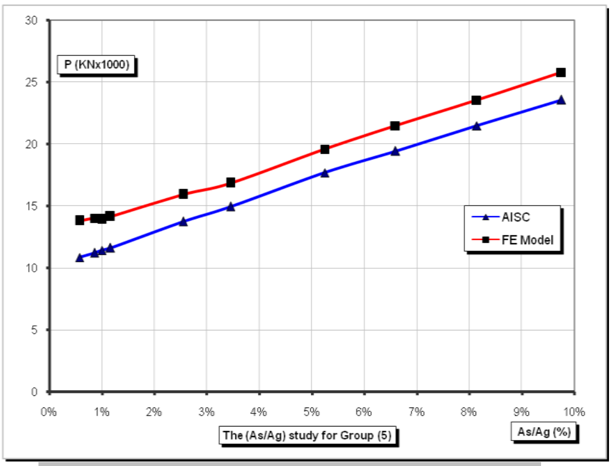

Figure (6) shows the result of study (A_s/A_g) for Group (5)

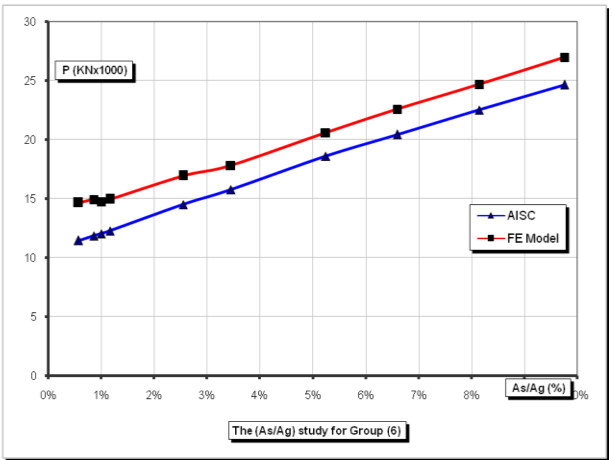

Figure (7) shows the result of study (A_s/A_g) for Group (6)

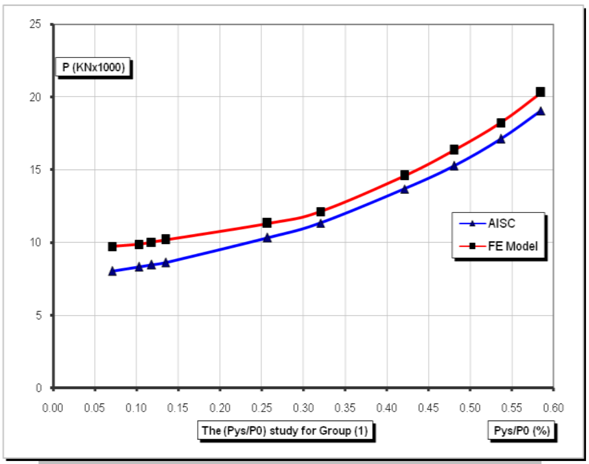

Figure (8) shows the result of study (P_{ys}/P_0) for Group (1)

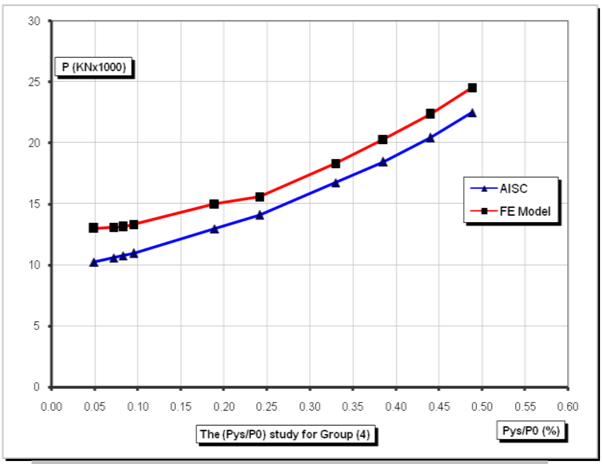

Figure (11) shows the result of study (P_{ys}/P_0) for Group (4)

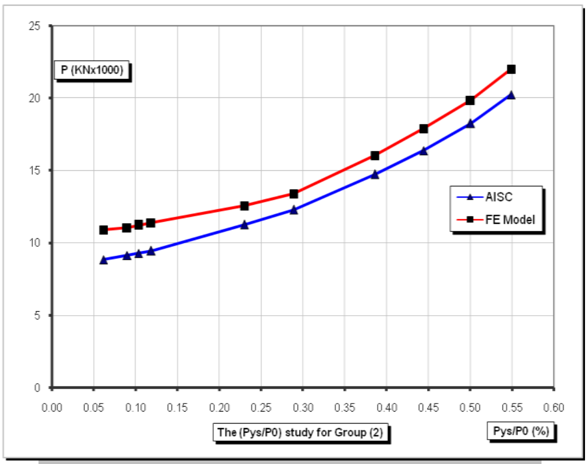

Figure (9) shows the result of study (P_{ys}/P_0) for Group (2)

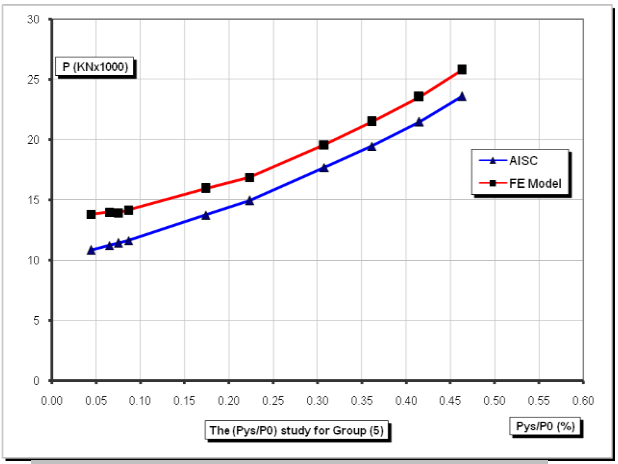

Figure (12) shows the result of study (P_{ys}/P_0) for Group (5)

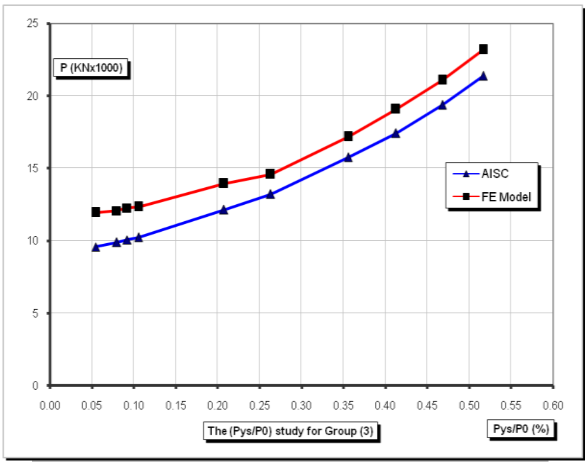

Figure (10) shows the result of study (P_{ys}/P_0) for Group (3)

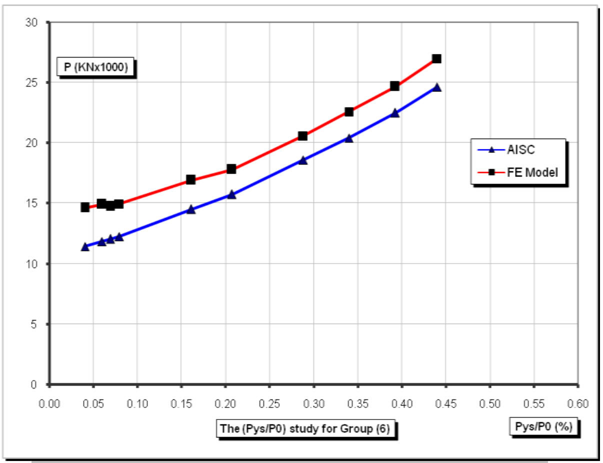

Figure (13) shows the result of study (P_{ys}/P_0) for Group (6)

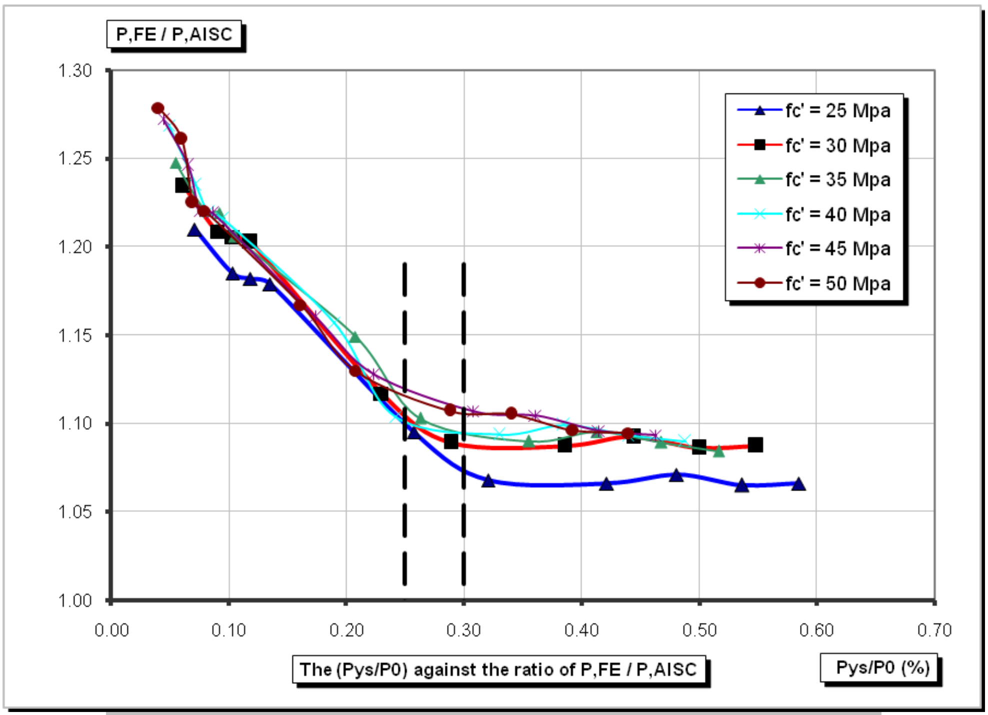

Figure (14) shows the result of study (P_{ys}/P_0) for all Groups in one graph

According to the figures of (A_s/A_g) against ($P_{,\ FE\ Model}$) & ($P_{n,AISC}$) it is observed that for all values of (A_s/A_g) more than certain limit, the curves of ($P_{n,\ AISC}$) were spaced constantly from the curves of ($P_{,\ FE\ Model}$). For the values of (A_s/A_g) less than this limit, the curves of the ($P_{n,\ AISC}$) were deviated from the curves of ($P_{,\ FE\ Model}$).

This limit is specifying the borderline for the range of application of the code. For the values of (A_s/A_g) more than this limit, the code results were matching with finite element results. However, for (A_s/A_g) values less than this limit the results of code were not matching with the finite element results.

The limit of (A_s/A_g) ranges from (1.9%) for group (1) to (4.2%) for group (6). Which means that limit differs from a group to another and the change in concrete strength and consequently the relative strength between steel core and concrete encasement will lead to change in the limit value.

The results of the figures (P_{ys}/P_0) against ($P_{,\ FE\ Model}$) & ($P_{n,AISC}$) is showing that there is a limit of (P_{ys}/P_0), For the values of (P_{ys}/P_0) more than this limit the results of the code are matching with the finite element results and beyond this limit the results of the code are not matching with finite element results. The limit of (P_{ys}/P_0) was the same for all groups and its value ranged between (0.25) to (0.3). Figure (4-16) illustrates the relations between (P_{ys}/P_0) and the normalized curves for ($P_{,\ FE\ Model}$ / $P_{n,\ AISC}$) and was leading to the same limit.

According to the AISC code this limit are specifying by the ratio of (A_s/A_g) and equals 1.0%. The results obtained from the finite element analysis were showing that the ratio of (A_s/A_g) are ignoring the effect of the relative strength of the steel core with respect to the strength of the concrete and steel reinforcement.

For more explanation, if there are two encased columns with the same (A_s/A_g) ratio and the steel core of the first column has a poor steel strength and the other column has a steel core with high steel strength and all the other parameters are the same. It is not accurate to assume that both columns will have the same classification against code limit of application regardless the effects of the relative strength. If we use the ratio of (P_{ys}/P_0) to specify the limit of codes application, it will consider the relative strength for the components of the encased sections.

IV. CONCLUSION AND RECOMMENDATIONS

From The results obtained, we can conclude the following:

- Specifying the limit on which the composite actions between the steel and concrete will start to be significant, cannot be accurate enough if we use a ratio of steel core area to the gross section area (A_s/A_g) as a reference.
- The ratio of the ultimate capacity of the steel core to the total ultimate capacity of the complete composite section (P_{ys}/P_0) will be efficiently representing this limit.
- It is suggested to change the limit of the ratio of steel core area to the gross section area (As/Ag) to be the ratio of the ultimate capacity of the

steel core to the total ultimate capacity of the complete composite section (P_{ys}/P_0).

- The limit for the ratio of (P_{ys}/P_0) can be specified with a value between (25 to 30%).

References

[1.] American Institute of Steel Construction (AISC-LRFD). (2005). Load and resistance factor design specification for steel building.
[2.] Dong Keon Kim, "A Database for composite columns", School of Civil and Environmental Engineering Georgia Institute of Technology, (2005).
[3.] Enrico Spacone and Sherif El-Tawil, "Nonlinear analysis of steel-concrete composite structures: State of the Art", Journal of Structural Engineering, 2004.
[4.] Joao Batista Marques de Sousa Jr. and Rodrigo Barreto Caldas, "Numerical Analysis of composite Steel-Concrete Columns of Arbitrary Section", Journal of Structural Engineering, 2005.
[5.] K. M. Yee, Dr H. Shakir-Khalil and R. Taylor, "Design Expressions for a New Type of Composite Column", Department of civil engineering, Simon Engineering laboratories, university of Manchester, 1982.
[6.] Min-Lang Lin and Keh-Chyuan Tsai, "Mechanical Behavior of Double-Skinned Composite Steel Tubular Columns", National center for research on earthquake engineering, Taipei, Taiwan, 2002.
[7.] Roberto t. Leon and Jerome f. Hajjar, "Limit State Response of Composite Columns and Beam-Columns", Journal of Structural Engineering, 2008.
[8.] S. A. Mirza, F. and E. A. Lacroix, "Comparative Strength Analyses of Concrete-Encased Steel Composite Columns", Journal of Structural Engineering, 2004.
[9.] S.F. Chen, J. G. Teng, and S. L. Chen, "Design of Biaxially Loaded Short Composite Columns of Arbitrary Section," Journal of Structural Engineering, 2001.
[10.] Sherif El-Tawil, and Gregory G. Deierlein, "Strength and Ductility of Concrete Encased Composite Columns", Journal of Structural Engineering, 1999.